Hindawi
Journal of Nanomaterials
Volume 2022, Article ID 3085103, 10 pages
https://doi.org/10.1155/2022/3085103

Research Article

Physicochemical Characterization and Viability Assays of a Promising Formulation of Liposomes (DODAB-DOPC) in Complexation with ctDNA

C. I. Ochoa-Sánchez,[1] K. Ochoa Lara,[2] J. M. Martínez-Soto,[3] A. Martínez-Higuera,[4] R. A. Iñiguez-Palomares,[1] R. Moreno-Corral,[2] E. Rodríguez-León,[1] A. Soto-Guzmán,[3] and C. Rodríguez-Beas[1]

[1]*Physics Department, University of Sonora, Rosales and Luis Encinas, 83000 Hermosillo, Sonora, Mexico*
[2]*Polymers and Materials Department, University of Sonora, Rosales and Luis Encinas, 83000 Hermosillo, Sonora, Mexico*
[3]*Medicine and Health Sciences Department, University of Sonora, Colosio and Reforma, 83000 Hermosillo, Sonora, Mexico*
[4]*Agriculture and Livestock Department, University of Sonora, Carretera a Bahia de Kino km 21, 305 Hermosillo, Sonora, Mexico*

Correspondence should be addressed to C. Rodríguez-Beas; cesar.rodriguez@unison.mx

Received 1 February 2022; Revised 13 May 2022; Accepted 7 June 2022; Published 25 June 2022

Academic Editor: Haseeb A. Khan

The search of new genetic vectors that improve the efficacy of gene delivery into diseased cells has led to the creation of several vector formulations that promote effectiveness in applications. However, DNA affinity to vectors as well as vector/DNA complex stability remains a problem to be solved. Here, we study lipoplexes made of DODAB-DOPC cationic liposomes (CL) and calf thymus DNA (ctDNA) as a preliminary cargo gene model of a novel vector formulation to improve DNA delivery efficacy and affinity. Physicochemical characterization was carried out by *Z*-potential (ζ), light scattering, ultraviolet, fluorescence spectra, confocal, and electronic microscopy to prove CL and ctDNA complexation and high affinity. Through this approach, ζ and light scattering results indicate an effective CL and ctDNA complexation; CL charge decreases as ctDNA concentration increases. Obtained spectra from UV and fluorescence show high affinity between CL and ctDNA. This can be also verified by confocal microscopy images and electronic microscopy micrographs. All experiments show effective binding between CL and ctDNA, and fluorescence experiments show EtBr displacing as CL concentration increments. CL cytotoxicity assays show high viability when ctDNA is complexed; these results are comparable with those obtained using Lipofectamine 2000. Easy complexation and low cytotoxicity make them a promising formulation for gene delivery. The obtained results from this work motivate us to keep searching for new genetic vector formulations, which could reduce its cytotoxic effect and improve its transfection efficiency, in addition to the low cost of production compared with some commercial products.

1. Introduction

Genetic material transfection is a technique that can be used to promote gene overexpression and silencing. In the gene therapy field, viruses are widely used as genetic material carriers because of their high internalization capability into cells; despite of this, viruses also present high cytotoxicity in both *in vivo* and *ex vivo*. In the last few decades, liposomes have gained importance due to their promising properties as drug delivery systems [1–4] and gene therapy for both gene expression and gene silencing [5–7]. Since the late 80's, several liposome formulations have been developed using combinations of ionic lipids and colipids with organic molecules and chemical compounds to improve liposome stability and internalization into the cell [8].

CL has been of great importance to carry DNA [6, 9–11], pDNA [11], and siRNA [12–15] into cells because of the easy interaction between them to form complexes, called lipoplexes, and this is the result of the electrostatic interaction between positively charged liposome and negatively

charged DNA. CL also exhibits less cytotoxicity than viral vectors [16] traditionally used, although this toxicity remains high to use them in clinic applications. Different formulations show a low toxic effect of CL on human cells, changing parameters such as lipid molar ratio or mixing them with organic molecules or other chemical compounds [17–19].

It is well known that liposomes with big sizes and high positive ζ have a negative influence on cell viability both *in vitro* and *ex vivo* [17]; however, liposomes with sizes around 100 nm and low positive ζ are desirables [20]. In fact, by ζ, it can be observed that lipoplex surface charge can change as ctDNA concentration changes, an important characteristic that helps lipoplexes to interact with cells [21–23].

In the first stage of our work, spherical DODAB-DOPC 50 : 50 (mw : mw) liposomes were made, and their physicochemical and morphological properties such as size, ζ, absorbance, and fluorescence and then cytotoxic effects of liposomes and their complexes were analyzed. ζ and size were previously studied in interaction with $Na_2B_{12}H_{11}SH$ by Awad et al. [24], and no information of morphological properties or cytotoxicity effects were reported.

Liposome and lipoplex cytotoxicity was evaluated by MTT assay on HUVEC, MDA-MB-231, and HeLa CCL-2 cell lines, where low toxicity is observed in all systems comparable to the results obtained by using a worldwide commercial liposomal formulation reference Lipofectamine 2000®. In this work, a promising CL formulation was characterized and tested.

2. Experimental Section

2.1. Materials. For liposome formulation, cationic dimethyldioctadecylammonium bromide (DODAB) and zwitterionic 1,2-dioleoyl-sn-glycero-3-phosphocholine (DOPC) phospholipids were used (Sigma-Aldrich). For confocal microscopy studies, 1,2-dioleoyl-sn-glycero-3-phosphoethanolamine-N-(7-nitro-2-1,3-benzoxadiazol-4-yl) (ammonium salt) (NBD-PE)-labeled phospholipids and 4′,6-diamidino-2-phenylindole dihydrochloride (DAPI) (Avanti Polar, USA) to dye DNA were employed. ctDNA (Sigma-Aldrich) as a cargo model was used without further purification. Phospholipids were dissolved in 4-(2-hydroxyethyl) piperazine-1-ethanesulfonic acid and sodium salt (HEPES) buffer (Sigma-Aldrich) at a concentration of 4 mM and pH = 7.4. Ethidium bromide (EtBr) was used for fluorescence studies at 2.53 μM.

2.2. Methods. Liposome solutions were prepared by mixing DODAB and DOPC at 50 : 50 molar ratio, and in some cases, 1% mol of NBD-DOPE was used in HEPES buffer (with ultrapure water (18 mS cm^{-1}, Millipore)). Preparation includes rotary evaporation and filtration by an extrusion method [25], using a polycarbonate membrane with nominal pores of 100 nm and above phospholipid transition temperature conditions. A ctDNA stock solution was prepared according to the manufacturer's protocol, without agitation, and stored at 4°C for one day before being used. Lipoplexes were made using a fixed liposome concentration (0.30 mM) by increasing ctDNA concentration [ctDNA] and under soft magnetic agitation to ensure ctDNA homogenization. For UV-Vis and fluorescence experiments, lipoplexes were prepared using a fixed [ctDNA] of 18.87 μg/mL and 1.83 μg/mL, respectively, increasing [CL] by adding aliquots of a stock solution of CL.

2.3. Dynamic Light Scattering. Liposome and lipoplex sizes were measured by dynamic light scattering (DLS) using Zetasizer Nano ZS (Malvern Instruments, UK) with a resolution of 0.5 nm and sensitivity of 0.1 ppm to 40% *w*/*v*. The instrument determines the size by first measuring the particles of Brownian motion in the samples using DLS and interpreting a size from this using of the established theory. The relationship between particle size and its speed due to Brownian motion is defined in the Stokes-Einstein equation.

$$D = \frac{K_B T}{6\pi\eta R}, \tag{1}$$

where D is the diffusion coefficient, K_B is the Boltzmann constant, T is the temperature of sample, η is the viscosity, and R is the hydrodynamic ratio, which represents the particle size in nm. Each sample was measured at room temperature (25°C) in triplicate to verify reproducibility.

2.4. Zeta Potential. ζ of liposome and lipoplex solutions were measured by using a Zetasizer Nano ZS (Malvern Instruments, UK). The instrument calculates the ζ by determining the electrophoretic mobility (μ_e) using Henry's equation [26].

$$\mu_e = \frac{2\varepsilon\zeta f(ka)}{3\eta}, \tag{2}$$

where ε, η, and $f(ka)$ denote the media dielectric constant, media viscosity, and Henry's function, respectively. Two values are generally used as approximations for $f(ka)$ determination, either 1.5 or 1.0. Electrophoretic determination of ζ is commonly made in aqueous solvent and moderate electrolyte concentration. $f(ka)$, in this case, takes the value 1.5 and is referred to as the classical Smoluchowski approximation [26].

$$\alpha = \varepsilon\frac{\zeta}{\eta}. \tag{3}$$

Samples were placed into a U-shaped folded capillary cell for ζ measurements. Each sample was measured at room temperature (25°C) in triplicate to verify reproducibility.

2.5. UV-Vis Spectroscopy. An Agilent 8435 (Agilent Technologies) diode array spectrophotometer was used to obtain the UV-Vis spectrum in a measurement range of 200-900 nm. A liposome sample solution concentration range was $1.0 \times 10^{-5} - 1.1 \times 10^{-4}\,M$, while for lipoplex concentrations, a fixed concentration of ctDNA was used (18.87 μg/mL) for

liposome concentration in a range of $5.96 \times 10^{-6} - 1.1 \times 10^{-4}\ M$.

According to the liposome and lipoplex UV-Vis spectra, a calibration curve was made and fitted with a linear approximation using the Beer-Lambert law.

$$A = \varepsilon C l, \tag{4}$$

where ε is the molar extinction coefficient, C is the solution concentration, and l is the optical path length (cell dimension in cm). For the samples, rectangular and transparent quartz cells were used, and the cuvettes were thermostated at 25°C through circulating water. All experiments were performed at least in triplicate to verify reproducibility.

2.6. Ethidium Bromide Displacement Assay. Fluorescence experiments were carried out as described elsewhere [27], on a PerkinElmer LS50B spectrofluorophotometer, at 25°C. Briefly, the interaction effect between liposomes and ctDNA-EtBr complex was studied by adding a certain amount of liposome stock solution into the solution of the ctDNA-EtBr complex ([ctDNA] = 1.83 μg/mL and [EtBr] = 2.53 μM). This technique is frequently employed as a complementary diagnostic tool for the identification of ctDNA binding to small liposomes and molecules [28, 29].

EtBr-bound ctDNA fluorescence spectrum was obtained using a 510 nm excitation wavelength. Liposome influence on ctDNA-EtBr complex was evaluated by monitoring the fluorescence emission spectrum changes, which also provided the quenching constant of the ctDNA lipoplex K_{sv} by employing Stern-Volmer's equation [26–30]:

$$\frac{I_0}{I} = K_{\mathrm{sv}}[Q] + 1, \tag{5}$$

where I_0 and I are the emission intensities in the absence and in the presence of the quencher, K_{sv} is the quenching constant, and $[Q]$ is the quencher (liposomes) concentration. K_{sv} is the slope obtained from I_0/I vs. Q plot.

2.7. Confocal Microscopy. Liposome and lipoplex micrograph analyses were carried out by a confocal laser scanning microscopy (CLSM) in an LSM800 device (Carl Zeiss, Jena, Germany), mounted on an inverted microscope Axio Observer Z1 (Carl Zeiss, Jena, Germany), and a Plan-Apochromatic 100x/1.40 oil objective was used. Two lasers of 405 and 488 nm, with respective maximum powers of 5 and 10 mW, were used for the study. Fluorescence was collected using highly sensitive GaAsP detectors. DAPI to label ctDNA and NBD-DOPE-labeled lipids were used as dyes, with 340/488 nm and 463/536 nm excitation/emission wavelengths, respectively. Fluorescence was detected in the range of 410-462 nm for DAPI and 490-565 nm for NBD, with 2.5% and 0.2% of maximum power laser excitation, respectively. Confocal dye images were collected on separated tracks using a time image integration of 74 s for each track. Both track images were integrated in a merged image. NDB was used at 1% of total phospholipid concentration.

2.8. Electron Microscopy. Liposome and lipoplex micrograph analyses were also carried out by a scanning electron microscopy (SEM), equipped with a field emission Jeol JSM-7800F. A negative staining method was used to visualize the sample size and shape using phosphotungstic acid (PTA) as a dyeing agent at 2%. 10 μL of sample was deposited on copper grids covered with a formvar-carbon film (Electron Microscopy Sciences, 300 Mesh), then 10 μL of PTA was added for 20 s, and the excess was removed. The grids were left to dry for 24 h at room temperature, and they were only covered to protect them from dust. All samples were measured at 5.0 kV in secondary electron (SE) mode.

2.9. Cell Viability Assays. To evaluate CL and lipoplex cytotoxicity (CL/ctDNA), viability was evaluated on cervical cancer (HeLa, CCL-2), human umbilical vein endothelial (HUVEC), and human breast cancer (MDA-MB-231) cell lines. HeLa CCL-2 cells were grown in Roswell Park Memorial Institute (RPMI-1640, Sigma-Aldrich), while HUVEC and MDA-MB-231 on Dulbecco's modified Eagle's medium (DMEM, Sigma-Aldrich). Both mediums were supplemented with 10% of fetal bovine serum (FBS), and cells were grown at 37°C and 5% of CO_2. For 3-(4,5-dimethylthiazolyl-2)-2,5-diphenyltetrazolium bromide (MTT) assays, all cell lines were adjusted to 5×10^4 cells/well in 96-well plates, and once the cells were attached, the treatments were added and incubated for 24 h. MTT assays were performed under the manufacturer's specifications (Sigma-Aldrich). Non-treated cells were set as controls. All viability assays were performed in triplicate. Also, cell viability assays were carried out using Lipofectamine 2000 and were used as it is usually referenced [31, 32].

Additionally, flow cytometry assays were performed employing calcein-AM (EMD Merck Millipore, USA) to the established cell viability. All cell lines were adjusted to 2.5×10^5/well in 12-well plates, and once cells were attached, the cells were serum-starved for 24 h and then treated and incubated with CL/ctDNA for 24 h. Positive viability control of cells without any treatment, CL alone, and the vehicle was performed. As a negative viability control, cells were 70°C treated for 20 min. After incubation, cells were harvested and resuspended in PBS. For calcein-AM staining, 2 μL of 50 μM calcein-AM solution was added and then incubated in the dark for 15 min. Cell viability was analyzed by flow cytometry. All treatments were done in triplicate to verify reproducibility, 10,000 events were acquired on a BD FACSVerse (Becton Dickinson) using BD FACSuite program (BD Biosciences), and one-way ANOVA determined statistical differences with Bonferroni's post hoc test. The obtained data were percentages of positive cells for calcein-AM staining in the FITC-A channel.

2.10. Statistical Analysis. One-way ANOVA with Tukey posttest analysis was used to determine the statistical significance ($p < 0.05$) of viability, using OriginPro 9.1 software, in the comparison between our liposomes and Lipofectamine 2000. Data are represented as the mean ± standard deviation (SD).

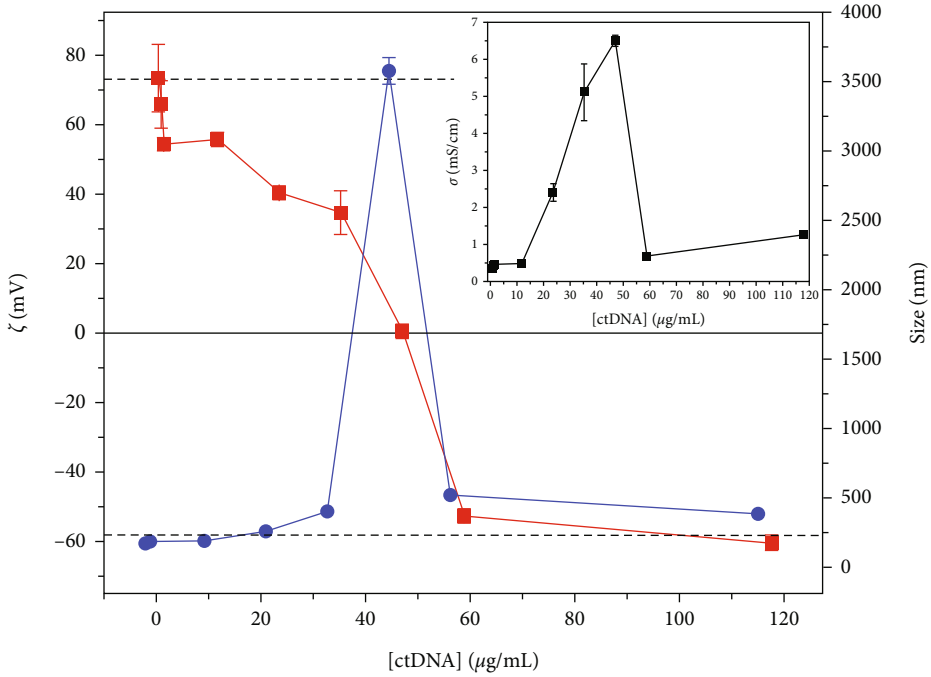

Figure 1: ζ (full square) and size (full circle) of lipoplexes as a function of [ctDNA]. Dashed and dotted lines represent the values of ζ (71 ± 1.55 mV) and size (170.2 ± 3.75 nm) of a fixed [CL alone] = 0.30 mM, respectively. Inset graph corresponds to σ of samples as [ctDNA] increases.

3. Results and Discussion

It is well known that mammalian cells possess a negatively charged plasmatic membrane, mainly due to the phospholipid negative natural charge [33]. It is also known that membrane neutral phospholipids help with stabilization, and otherwise, lacking this type of phospholipids can cause a disorder, e.g., atherosclerosis [34]. In this sense, phospholipid nature plays an essential role on liposome physicochemical behavior. CL has a great attention in studies focused on the search for new nonviral vehicles, whose physicochemical characteristics, such as size, charge, and interaction with other molecules, continue to be of great importance, as well as the cell transfection process.

3.1. Zeta Potential and Size. ζ is a parameter of great importance in lipoplex formation. Interactions between CL and ctDNA are described in terms of ζ, size, and conductivity changes. Figure 1 shows ζ changes in lipoplex formation as a function of [ctDNA] and for a fixed [CL] (0.30 mM). As can be seen, before adding ctDNA, CL ζ is 71 ± 2 mV and ζ decreases as ctDNA concentration increases, showing three ζ regions: (i) positive region, where the net charge is governed by CL, i.e., CL/ctDNA charge ratio is >1, because CL is the solution major component; (ii) neutral region (isoelectric point), where charge ratio = 1 (number of lipid charges and number of DNA-free phosphates are "equals"), resulting in a lipoplex aggregation; and (iii) negative region, where CL/ctDNA charge ratio is <1, and negative charge of ctDNA reigns due to the number of free ctDNA phosphates in a solution that overcomes the CL positively charged groups. These ζ regions' behavior is also described by Rodríguez-Pulido et al. [35], to a fixed [ctDNA] and variable [CL], indicating the binding between CL and ctDNA with lipoplex formation. Figure 1 also shows lipoplex size as [ctDNA] increases. According to the ζ regions, at the lowest [ctDNA], the size of the formed lipoplexes matched with the size of uncomplexed CL (170 ± 4 nm). As [ctDNA] increases, lipoplex size increases in agreement with ζ that it is in the isoelectric point region, where lipoplexes reduce electrostatic repulsion resulting in aggregate formation. When the ctDNA charge dominates, the electrostatic repulsion force plays again an important role in lipoplex interactions and lipoplex size, at the beginning of their formation, at the lower [ctDNA].

According to fabricant's recommendations for Lipofectamine 2000® concentrations for transfection or cytotoxicity assays, Lipofectamine 2000® shows sizes of 98 ± 3 nm and a ζ = 13.7 ± 3.5 mV, fixing [Lipofectamine 2000]; three different concentrations of ctDNA were tested, starting from fabricant's recommended DNA concentration of 0.2 μg/well and then 0.5 μg/well and 1 μg/well. For [ctDNA] = 0.2 μg/well, lipoplexes show aggregates of 3974 ± 204 nm and ζ = 0.42 ± 1.3 mV, i.e., isoelectric point for Lipofectamine 2000® sizes of 189 ± 1 nm and ζ = −28.3 ± 1.4 mV for the highest ctDNA concentration.

Conductivity data also were taken from ζ measurements in lipoplex formation analysis. The inset plot in Figure 1 shows the solution conductivity as [ctDNA] increases. The graph also presents an abrupt change in the behavior for the same [ctDNA], in which the isoelectric point is reached in the ζ measurements. Rodríguez-Pulido et al. [35] justify

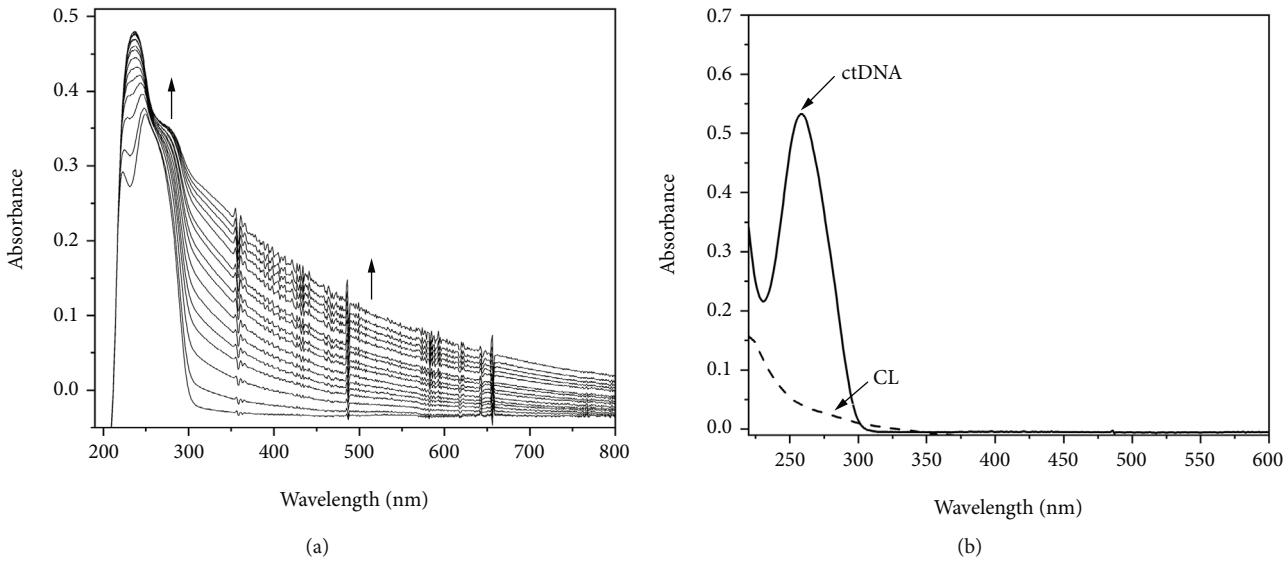

Figure 2: (a) UV-Vis variation of absorption spectra for ctDNA (18.87 μg/mL) solution upon addition of liposomes ($0 - 1.1 \times 10^{-4}$ M) and (b) absorption spectra for solutions of ctDNA (18.87 μg/mL) and liposomes (1.1×10^{-4} M). Both solutions were in HEPES buffer pH = 7.4, at 25°C.

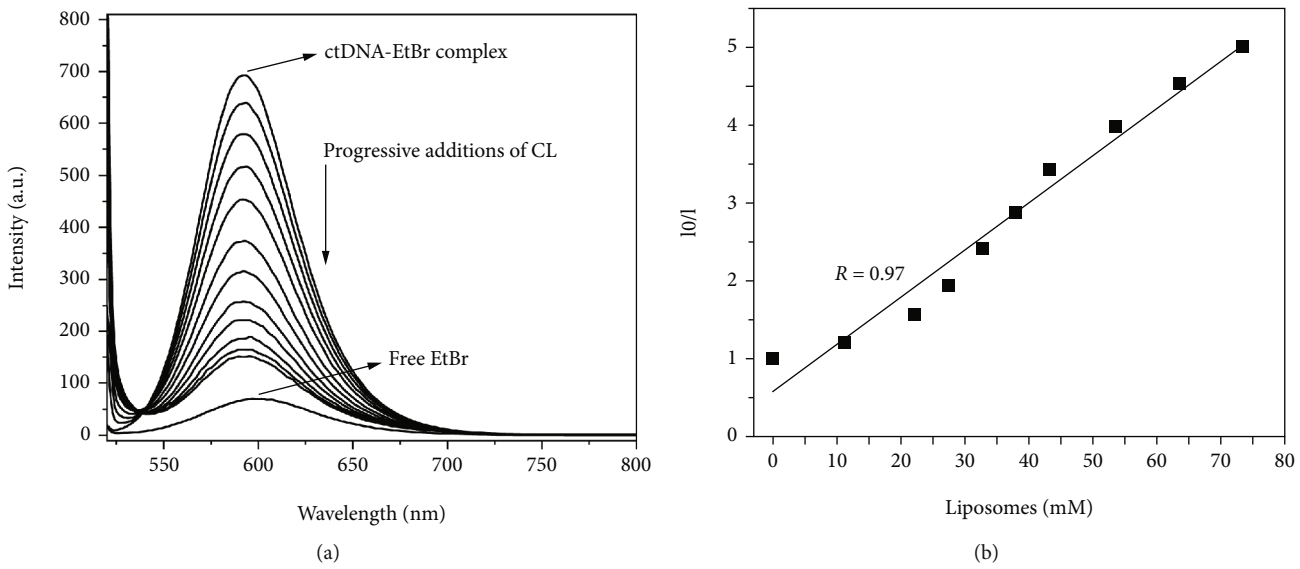

Figure 3: (a) Displacement assays of emission spectra of ctDNA-EtBr complex in the presence of liposomes, $\lambda_{exc} = 510$ nm, in HEPES buffer, pH = 7.4. [EtBr] = 2.53 μM, [ctDNA] = 1.83 μg/mL, and [liposomes] = 0 – 80 μM. (b) The Stern-Volmer plot of the fluorescence titration of ctDNA-EtBr with liposomes.

this conductivity increase because of lipoplex formation, which induces a counterion release, i.e., Na^+ from ctDNA and Br^- from CL.

3.2. UV-Vis Spectra. CL-ctDNA lipoplexes in HEPES buffer (pH 7.4) were studied by titration experiments and monitored by UV-Vis spectroscopy. Previously, ctDNA stability was verified for 7 h at 25°C in HEPES buffer at pH = 7.4 (Figure S1 of the Supplementary Materials). Regarding these experiments, it was found that upon liposomes, addition to a ctDNA (18.87 μg/mL) solution, induced significant changes in absorbance, with a maximum increase and with absorption baseline elevation (see Figure 2(a)). This effect may be attributed undoubtedly to ctDNA lipoplex formation because ctDNA and liposome solutions separately do not behave with baseline elevation (see Figure 2(b)). In this respect, the association of CL with ctDNA via electrostatic interactions can be expected to produce a hydrophobic lipoplex [36, 37].

3.3. Ethidium Bromide Displacement Assay. ctDNA affinity to CL was evaluated through EtBr displacement assay by fluorescence spectroscopy. All experiments gave significant changes in the fluorescence emission, which allowed their reproduction with accuracy, and therefore, this technique is appropriate for studying the lipoplex in solution. Typical

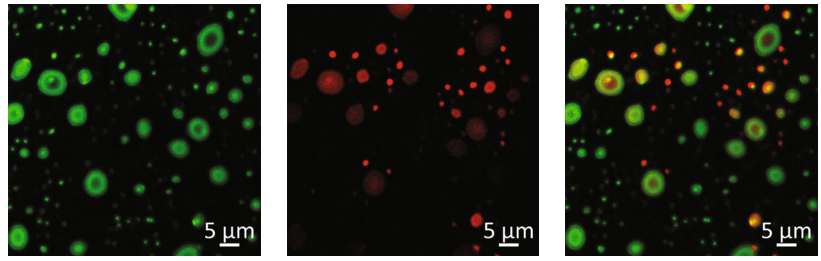

(a) (b) (c)

Figure 4: NBD fluorescence (a) and DAPI fluorescence (b) captured by confocal in double-labeled lipoplex samples. (c) Merged micrographs of NBD and DAPI fluorescence micrographs. For DAPI emission, a false red color was used to improve the contrast in the merged micrograph.

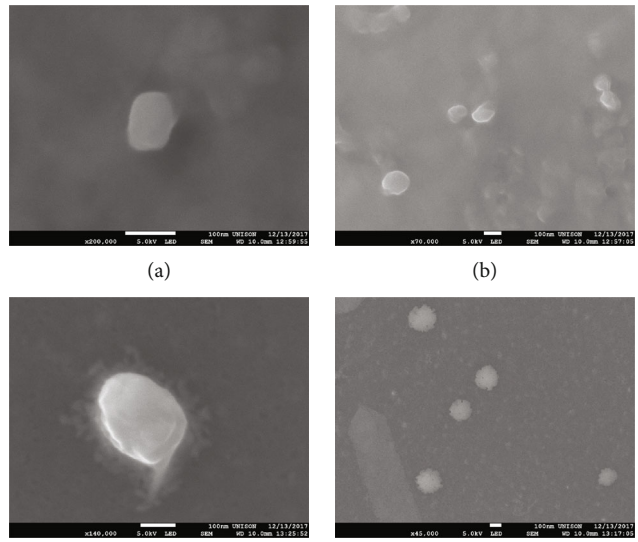

(a) (b) (c) (d)

Figure 5: Scanning electron microscopy micrographs (SE mode) of an individual liposome (a) and liposome group at low magnification (b). An individual lipoplex micrograph is shown in (c) and (d) corresponds to lipoplex group. ctDNA concentration of lipoplex samples was 35.30 μg/mL.

changes in the emission spectra of EtBr bound to ctDNA ([EtBr] = 2.53 μM and [ctDNA] = 1.83 μg/mL) upon titration with the liposome are shown in Figure 3(a). By simple inspection of the graph in this figure, it is evident that liposome addition causes an appreciable reduction in ctDNA-EtBr complex fluorescence intensity, corresponding to 80.25% of ctDNA-EtBr complex intensity. Quenching data analysis by the Stern-Volmer equation (defined above) gave a K_{sv} value of $5.9 \times 10^5\ M^{-1} \pm 0.1 \times 10^5$ (Figure 3(b)). This gives evidence that liposomes can effectively replace EtBr from ctDNA-EtBr complex due to the formation of a more stable ctDNA lipoplex. K_{sv} value implies a very good affinity of ctDNA towards CL and it could also help to determine the optimal concentration of CL necessary for *in vitro* transfection [38, 39].

3.4. Confocal Microscopy. ctDNA (35.30 μg/mL) interaction with CL (0.33 mM) was analyzed by CLSM. Labeled phospholipid NBD-DOPE (1 : 100 molar ratio) was used to fabricate fluorescent liposomes and DAPI-labeled ctDNA. According to the microscope resolution, bigger liposome sizes were used than those used in the previous techniques, assuming that the complexation process is independent of the liposome size. Figure 4 shows images that correspond to NBD-labeled liposomes (green) (Figure 4(a)), ctDNA labeled with DAPI (red) (Figure 4(b)), and the merged images corresponding to both NBD and DAPI emissions (Figure 4(c)). In the images, it is observed that in the regions where the NBD emits, there is also a DAPI emission, proving that ctDNA is indeed linked to the liposome surface. Each emission was taken in separated channels to avoid self-excitation due to multiple dyes. Micrographs clearly show regions where NBD and DAPI emissions match, proving that ctDNA is indeed complexed to CL surface. ctDNA is not homogeneously distributed in all liposomes despite following the protocol; a similar behavior was reported by Gordon et al. [40]. Cationic LUVs/ctDNA complexes were previously separated by centrifugation, following Güven et al.'s protocol [41].

3.5. Electron Microscopy. Due to CLSM resolution and the CL size, when ctDNA was complexed on the liposome surface, apparently it does not modify lipoplex size. While in DLS size measurements, lipoplex size increased as

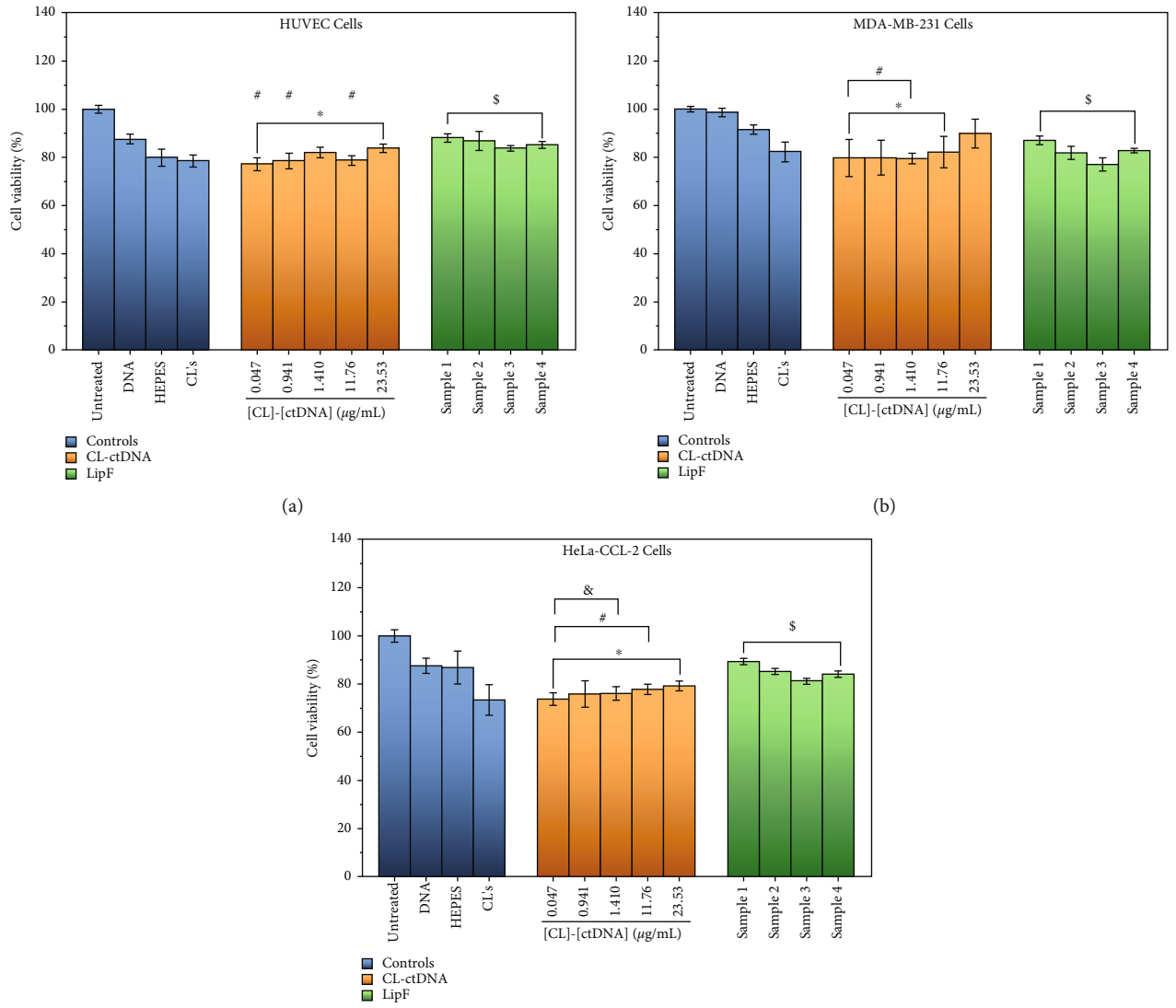

Figure 6: Cytotoxicity assays on HUVEC, MDA-MB-231, and HeLa CCL-2 cell lines. Names on bars indicate samples and concentrations for each cell line, as follows (from left to right): (bar 1) cell control [5×10^4 cells/well]; (bar 2) fixed [ctDNA alone] = 80 μg/mL; (bar 3) fixed [HEPES buffer alone] = 4 mM; (bar 4) fixed [CL alone] = 30 μM; (bar 5) [CL] – [ctDNA] = 0.04705 ng/μL; (bar 6) [CL] – [ctDNA] = 0.941 μg/mL; (bar 7) [CL] – [ctDNA] = 1.41 μg/mL; (bar 8) [CL] – [ctDNA] = 11.76 μg/mL; (bar 9) [CL] – [ctDNA] = 23.53 μg/mL; (bar 10) fixed [Lipofectamine 2000 alone] = 0.5 μL/well; (bar 11) [Lipofectamine 2000] – [ctDNA] = 0.2 μg/well; (bar 12) [Lipofectamine 2000] – [ctDNA] = 0.5 μg/well; (bar 13) [Lipofectamine 2000] – [ctDNA] = 1 μg/well.

[ctDNA] increased. To compare the increase in the size of lipoplex, SEM was used, since this technique allows to clearly observe liposomes with sizes around 100 nm. Filtered liposomes (0.33 mM) were observed using a 100 nm pore size disc filter and following a negative stain protocol described before. Figures 5(a) and 5(b) show CL micrographs, where CL surface contour can be observed. Figures 5(c) and 5(d) show lipoplex micrographs, where molecules are attached to liposomes, which give a surface irregularity. An individual lipoplex is shown in Figure 5(c), where it can see the complex surface. A size increase is observed from approximately 91 nm (average size of CL alone) to 219 nm. Accordingly, in all previous experiments, SEM results also showed a binding between CL and ctDNA, increasing the formed lipoplex size as [ctDNA] increases. Similar results were observed by Zhang et al. [42] and Rasoulianboroujeni et al. [43] in their liposome-DNA complexation study, where DNA is strongly associated with liposomes. It is important to mention that lipoplexes with these same characteristics were used in cellular viability assays.

3.6. Cell Viability Assays. CL and lipoplex cytotoxicity was tested in HUVEC, MDA-MB-231, and HeLa CCL-2 cell lines by MTT assays. For these assays, fixed concentrations of CL (0.30 mM) and ctDNA (80 μg/mL) in HEPES buffer (4 mM) were used as controls, and five ctDNA concentrations between 0.043 and 23.53 μg/mL were tested. Figure 6 shows CL and lipoplex viability assays and different

[ctDNA]. On HUVEC cells, taken as a healthy model of cells, CL shows low toxicity, reporting around 80% of viability, while the lowest toxicity effect is observed in MDA-MB-231 cells with 82.3 ± 3.9% of viability. As a control, CL alone showed the highest toxicity on HeLa CCL-2 cells with a viability of 73.3 ± 6.2%. In general, lipoplexes showed a viability around 80% for HUVEC, 83% for MDA-MB-231, and 76% for HeLa CCL-2. A similar synergistic effect was reported by Nguyen et al. using CL and plasmid DNA in HeLa, B16BL6, and RGC-6 cell lines [44]. In our case, a higher viability for lipoplexes was observed for the highest [ctDNA] used (2.18 μg/mL), compared with the other CL/ctDNA formulations. CL used as a base for lipoplex shows high cell viability in the tested cell lines, reporting a maximum toxicity of 27% on HeLa cells and close to 20% for most of the cases. To compare cytotoxicity effects, Lipofectamine 2000 was employed as a reference following the fabricant's protocol and concentrations, the results showing similar cytotoxicity levels at concentrations between Lipofectamine 2000 using 3 [ctDNA] around fabricant's recommendation and CL. Due to this low toxicity, their easy complexation with DNA, high stability (see Figure 1), and low-cost lipids, compared with other anionic formulations commonly used, makes them a promising nonviral vector for gene delivery.

Statistically significant differences between the untreated cell control and [CL] − [ctDNA] = [0.04705 − 23.53 μg/mL] are indicated in Figure 6 by ∗, between fixed [ctDNA alone] = 80 μg/mL and [CL] − [ctDNA] = [0.04705 − 23.53] μg/mL are indicated by #, and between fixed [HEPES buffer alone] = 4 mM and [CL] − [ctDNA] = [0.04705 − 23.53 μg/mL] are indicated by &. Nonsignificant differences are not indicated. We are using Lipofectamine 2000 as a commercialized positive control, and significant differences with respect to the untreated cell control are indicated by $. In general, all these values show a statistical significance ($p < 0.05$).

Additionally, calcein-AM detection by flow cytometry was performed to assess if the viability of HUVEC, MDA-MB-231, and HeLa-CCL-2 cell lines is affected by [CL]-[ctDNA] at different concentrations. For that, CL alone (0.30 mM), ctDNA (80 μg/mL), and HEPES buffer (4 mM) were used as controls ($p > 0.05$); cells treated by 20 min at 70°C were negative controls of viability compared to the untreated cells ($p < 0.0001$) (see Figure S2 of the Supplementary Materials). Four [CL]-[ctDNA] concentrations between 0.047 and 11.76 μg/mL were tested. Figure S2 shows that the viability at different [CL]-[ctDNA] was not statistically affected compared to the untreated cells; [CL]-[ctDNA]-treated HUVEC cells show around 91% of viability ($p > 0.05$), MDA-MB-231-treated cells show around 95% of viability ($p > 0.05$), and HeLa-CCL-2 cells show around 93% of viability ($p > 0.05$). We also include in the supplementary information the raw data from the flow cytometry measurements of each of the cell lines (Figures S3, S4, S5, and S6), which we used to construct the bar graph (Figure S2).

These data and the cytotoxicity assays evaluated by MTT allow us to affirm that these lipoplexes do not affect cell line viability, making them good candidates for use as molecular vectors.

4. Conclusions

DODAB-DOPC CL is a promising formulation due to the easy way to form complexes with ctDNA. The different experimental techniques confirm that this complexation occurs easily. EtBr displacement assay shows a good affinity between CL and ctDNA. Cell viability assays show positive results due to the low toxicity of the tested formulations, compared to the low toxicity produced by commercial CL Lipofectamine 2000. As said before, CL easy complexation with ctDNA, high stability, and low-cost lipids, compared with other anionic formulations commonly used, makes this formulation a promising nonviral vector for gene delivery or drug delivery systems. Internalization pathways of this formulation must be studied to find ways to enhance cell transfection.

Data Availability

All data used to support the findings of this study are included within the article and supplementary material.

Conflicts of Interest

The authors declare that they have no conflicts of interest regarding the publication of this paper.

Acknowledgments

C.I. O-S thanks CONACYT (Mexico) for his scholarship number (446287). C.I. O-S, A. M-H, R.A. I-P, E. R-L, and C. R-B thank to the laboratories of Biomaterials and Scanning Microscopy, Department of Physics of the University of Sonora for micrographs.

Supplementary Materials

Figure S1: ctDNA stability measurements over time by (A) UV-Vis and (B) fluorescence. The measurements were recorded for 7 h at 25°C in HEPES buffer at pH = 7.4. Figure S2: calcein-AM viability assays. Flow cytometry measurements of viability in (A) HUVEC, (B) MDA-MB-231, and (C) HeLa-CCL-2 cell lines were performed by triplicate using calcein-AM according to the classification strategy described in Figure S3. The graph represents the mean ± SD of three independent experiments, expressed as cell viability (%). Culture conditions are indicated in the below bars: the untreated cells as control of viability [2.5×10^5 cells/well]; ctDNA [80 mg/mL ctDNA alone-treated cells]; death control [70°C/20 min-treated cells]; 4 mM HEPES-treated cells; [CL] 0.133 mM-treated cells; and [CL]-[ctDNA]-treated cells. ∗∗∗∗ denotes $p < 0.0005$ compared to the untreated cells (one-way ANOVA with Bonferroni's post hoc test). Figure S3: calcein-AM configuration. A representative analysis of the cell lines in BD FACSVerse, gating cells by (B) forward scatter (FSC), (C) side scatter (SSC), and (D) gating of positive calcein-AM cells in FITC-A (B4). 10,000 events in (D) for calcein-AM expression were detected. Figure S4: HUVEC cell viability by FACS using calcein-AM. A representative dot plot of calcein-AM

viable cell detection in HUVECs is shown. 10,000 events in (D) for calcein-AM expression (FITC-A channel) were detected (Figure S3(D)). Gated cells into dot plots are calcein-AM-positive viable cells (A), positive viability control (untreated cells) (B), vehicle control (CL alone-treated cells) (C), buffer control (HEPES) (D), ctDNA control (ctDNA alone-treated cells) (E), and [CL]-[ctDNA]-treated cells C1 (0.047 μg/mL) (F), C2 (0.941 μg/mL) (G), C3 (1.410 μg/mL) (H), and C4 (11.76 μg/mL) (I). Figure S5: MDA-MB-231 cell viability by FACS using calcein-AM. A representative dot plot of calcein-AM detection in MDA-MB-231cells. 10,000 events in (D) for calcein-AM expression (FITC-A channel) were detected (Figure S3(D)). Gated cells into dot plots are calcein-AM-positive viable cells (A), positive viability control (untreated cells) (B), vehicle control (CL alone-treated cells) (C), buffer control (HEPES) (D), ctDNA control (ctDNA alone-treated cells) (E), and [CL]-[ctDNA]-treated cells C1 (0.047 μg/mL) (F), C2 (0.941 μg/mL) (G), C3 (1.410 μg/mL) (H), and C4 (11.76 μg/mL) (I). Figure S6: HeLa-CCL-2 cell viability by FACS using calcein-AM. A representative dot plot of calcein-AM detection in HeLa-CCL-2 cells is shown. 10,000 events in (D) for calcein-AM expression (FITC-A channel) were detected (Figure S3(D)). Gated cells into dot plots are calcein-AM-positive viable cells (A), positive viability control (untreated cells) (B), vehicle control (CL alone-treated cells) (C), buffer control (HEPES) (D), ctDNA control (ctDNA alone-treated cells) (E), and [CL]-[ctDNA]-treated cells C1 (0.047 μg/mL) (F), C2 (0.941 μg/mL) (G), C3 (1.410 μg/mL) (H), and C4 (11.76 μg/mL) (I). *(Supplementary Materials)*

References

[1] P. Qi, M. Cao, L. Song et al., "The biological activity of cationic liposomes in drug delivery and toxicity test in animal models," *Environmental Toxicology and Pharmacology*, vol. 47, pp. 159–164, 2016.

[2] K. B. Knudsen, H. Northeved, P. K. Ek et al., "In vivo toxicity of cationic micelles and liposomes," *Nanomedicine: Nanotechnology, Biology, and Medicine*, vol. 11, no. 2, pp. 467–477, 2015.

[3] M. Sugano, H. Morisaki, Y. Negishi et al., "Potential effect of cationic liposomes on interactions with oral bacterial cells and biofilms," *Journal of Liposome Research*, vol. 26, no. 2, pp. 156–162, 2016.

[4] X. Gai, L. Cheng, T. Li et al., "In vitro and in vivo studies on a novel bioadhesive colloidal system: cationic liposomes of ibuprofen," *AAPS PharmSciTech*, vol. 19, no. 2, pp. 700–709, 2018.

[5] Y. Hattori, Y. Machida, M. Honda et al., "Small interfering RNA delivery into the liver by cationic cholesterol derivative-based liposomes," *Journal of Liposome Research*, vol. 27, no. 4, pp. 264–273, 2017.

[6] E. Junquera and E. Aicart, "Cationic lipids as transfecting agents of DNA in gene therapy," *Current Topics in Medicinal Chemistry*, vol. 14, no. 5, pp. 649–663, 2014.

[7] R. N. Majzoub, K. K. Ewert, and C. R. Safinya, "Cationic liposome-nucleic acid nanoparticle assemblies with applications in gene delivery and gene silencing," *Philosophical Transactions. Series A, Mathematical, Physical, and Engineering Sciences*, vol. 374, no. 2072, p. 20150129, 2016.

[8] Y.-M. Zhang, Z. Huang, J. Zhang, W.-X. Wu, Y.-H. Liu, and X.-Q. Yu, "Amphiphilic polymers formed from ring-opening polymerization: a strategy for the enhancement of gene delivery," *Biomaterials Science*, vol. 5, no. 4, pp. 718–729, 2017.

[9] S. A. Tatarkova and S. Khaira, "Characterization of liposomes for cancer cell transfection," *The Open Biomedical Engineering Journal*, vol. 1, no. 1, pp. 60–63, 2007.

[10] A. Rodríguez-Pulido, E. Aicart, O. Llorca, and E. Junquera, "Compaction process of calf thymus DNA by mixed cationic-zwitterionic liposomes: a physicochemical study," *The Journal of Physical Chemistry. B*, vol. 112, no. 7, pp. 2187–2197, 2008.

[11] B. Ruozi, F. Forni, R. Battini, and M. A. Vandelli, "Cationic liposomes for gene transfection," *Journal of Drug Targeting*, vol. 11, no. 7, pp. 407–414, 2003.

[12] D. Yang, Y. Li, Y. Qi et al., "Delivery of siRNA using cationic liposomes incorporating stearic acid-modified Octa-arginine," *Anticancer Research*, vol. 36, no. 7, pp. 3271–3276, 2016.

[13] Y. Hattori, A. Nakamura, S. Arai, K. Kawano, Y. Maitani, and E. Yonemochi, "siRNA delivery to lung-metastasized tumor by systemic injection with cationic liposomes," *Journal of Liposome Research*, vol. 25, no. 4, pp. 279–286, 2015.

[14] A. Lechanteur, V. Sanna, A. Duchemin, B. Evrard, D. Mottet, and G. Piel, "Cationic liposomes carrying siRNA: impact of lipid composition on physicochemical properties, cytotoxicity and endosomal escape," *Nanomaterials*, vol. 8, no. 5, 2018.

[15] F. Haghiralsadat, G. Amoabediny, S. Naderinezhad, T. Forouzanfar, M. N. Helder, and B. Zandieh-Doulabi, "Preparation of PEGylated cationic nanoliposome-siRNA complexes for cancer therapy," *Artificial Cells, Nanomedicine, and Biotechnology*, vol. 46, no. sup1, pp. 684–692, 2018.

[16] B. Wetzer, G. Byk, M. Frederic et al., "Reducible cationic lipids for gene transfer," *The Biochemical Journal*, vol. 356, no. 3, pp. 747–756, 2001.

[17] H. Lv, S. Zhang, B. Wang, S. Cui, and J. Yan, "Toxicity of cationic lipids and cationic polymers in gene delivery," *Journal of Controlled Release*, vol. 114, no. 1, pp. 100–109, 2006.

[18] J. Ju, M.-L. Huan, N. Wan, H. Qiu, S.-Y. Zhou, and B.-L. Zhang, "Novel cholesterol-based cationic lipids as transfecting agents of DNA for efficient gene delivery," *International Journal of Molecular Sciences*, vol. 16, no. 12, pp. 5666–5681, 2015.

[19] J. Lewandowska-Łańcucka, K. Mystek, A. Gilarska et al., "Silicone-stabilized liposomes as a possible novel nanostructural drug carrier," *B, Biointerfaces*, vol. 143, pp. 359–370, 2016.

[20] C. Madeira, L. M. S. Loura, M. R. Aires-Barros, and M. Prieto, "Fluorescence methods for lipoplex characterization," *Biochimica et Biophysica Acta*, vol. 1808, no. 11, pp. 2694–2705, 2011.

[21] L. Kudsiova, A. Mohammadi, M. F. M. Mustapa et al., "Trichain cationic lipids: the potential of their lipoplexes for gene delivery," *Biomaterials Science*, vol. 7, no. 1, pp. 149–158, 2019.

[22] T. Andey, N. Bora-Singhal, S. P. Chellappan, and M. Singh, "Cationic lipoplexes for treatment of cancer stem cell-derived murine lung tumors," *Nanomedicine: Nanotechnology, Biology, and Medicine*, vol. 18, pp. 31–43, 2019.

[23] H. Ando, A. S. Abu Lila, M. Fukushima et al., "A simplified method for manufacturing RNAi therapeutics for local administration," *International Journal of Pharmaceutics*, vol. 564, pp. 256–262, 2019.

[24] D. Awad, I. Tabod, S. Lutz, H. Wessolowski, and D. Gabel, "Interaction of Na2B12H11SH with liposomes: influence on

zeta potential and particle size," *Journal of Organometallic Chemistry*, vol. 690, no. 11, pp. 2732–2735, 2005.

[25] F. J. Martin and J. K. Morano, "Liposome extrusion method," *12*, 1988, US Patent. https://patents.google.com/patent/US4737323A/en.

[26] A. Malvern, *Zetasizer Nano User Manual*, Malvern Instruments Ltd, England, 2009.

[27] Y. Xu, S. W. Hui, P. Frederik, and F. C. Szoka Jr., "Physicochemical characterization and purification of cationic lipoplexes," *Biophysical Journal*, vol. 77, no. 1, pp. 341–353, 1999.

[28] Y. Xu and F. C. Szoka Jr., "Mechanism of DNA release from cationic liposome/DNA complexes used in cell transfection," *Biochemistry*, vol. 35, no. 18, pp. 5616–5623, 1996.

[29] V. Calvillo-Páez, R. R. Sotelo-Mundo, M. Leyva-Peralta et al., "Synthesis, spectroscopic, physicochemical and structural characterization of tetrandrine-based macrocycles functionalized with acridine and anthracene groups: DNA binding and anti-proliferative activity," *Chemico-Biological Interactions*, vol. 286, pp. 34–44, 2018.

[30] E. A. Permyakov, *Luminescent Spectroscopy of Proteins*, CRC Press, 2018.

[31] O. Paecharoenchai, N. Niyomtham, A. Apirakaramwong et al., "Structure relationship of cationic lipids on gene transfection mediated by cationic liposomes," *AAPS PharmSciTech*, vol. 13, no. 4, pp. 1302–1308, 2012.

[32] H. K. Dhaliwal, Y. Fan, J. Kim, and M. M. Amiji, "Intranasal delivery and transfection of mRNA therapeutics in the brain using cationic liposomes," *Molecular Pharmaceutics*, vol. 17, no. 6, pp. 1996–2005, 2020.

[33] F. Sakurai, T. Nishioka, H. Saito et al., "Interaction between DNA-cationic liposome complexes and erythrocytes is an important factor in systemic gene transfer via the intravenous route in mice: the role of the neutral helper lipid," *Gene Therapy*, vol. 8, no. 9, pp. 677–686, 2001.

[34] W. E. Connor, "Importance of n-3 fatty acids in health and disease," *The American Journal of Clinical Nutrition*, vol. 71, no. 1, pp. 171S–175S, 2000.

[35] A. Rodríguez-Pulido, A. Martín-Molina, C. Rodríguez-Beas, O. Llorca, E. Aicart, and E. Junquera, "A theoretical and experimental approach to the compaction process of DNA by dioctadecyldimethylammonium bromide/zwitterionic mixed liposomes," *The Journal of Physical Chemistry. B*, vol. 113, no. 47, pp. 15648–15661, 2009.

[36] L. Xu and T. J. Anchordoquy, "Cholesterol domains in cationic lipid/DNA complexes improve transfection," *Biochimica et Biophysica Acta*, vol. 1778, no. 10, pp. 2177–2181, 2008.

[37] M. T. Kennedy, E. V. Pozharski, V. A. Rakhmanova, and R. C. MacDonald, "Factors governing the assembly of cationic phospholipid-DNA complexes," *Biophysical Journal*, vol. 78, no. 3, pp. 1620–1633, 2000.

[38] Q.-D. Huang, G. X. Zhong, Y. Zhang et al., "Cyclen-based cationic lipids for highly efficient gene delivery towards tumor cells," *PLoS One*, vol. 6, no. 8, article e23134, 2011.

[39] Q. Liu, Q. Q. Jiang, W. J. Yi et al., "Novel imidazole-functionalized cyclen cationic lipids: synthesis and application as non-viral gene vectors," *Bioorganic & Medicinal Chemistry*, vol. 21, no. 11, pp. 3105–3113, 2013.

[40] S. P. Gordon, S. Berezhna, D. Scherfeld, N. Kahya, and P. Schwille, "Characterization of interaction between cationic lipid-oligonucleotide complexes and cellular membrane lipids using confocal imaging and fluorescence correlation spectroscopy," *Biophysical Journal*, vol. 88, no. 1, pp. 305–316, 2005.

[41] A. Güven, M. Ortiz, M. Constanti, and C. K. O'Sullivan, "Rapid and efficient method for the size separation of homogeneous fluorescein-encapsulating liposomes," *Journal of Liposome Research*, vol. 19, no. 2, pp. 148–154, 2009.

[42] Y.-M. Zhang, Y.-H. Liu, J. Zhang, Q. Liu, Z. Huang, and X.-Q. Yu, "Cationic gemini lipids with cyclen headgroups: interaction with DNA and gene delivery abilities," *RSC Advances*, vol. 4, no. 83, pp. 44261–44268, 2014.

[43] M. Rasoulianboroujeni, G. Kupgan, F. Moghadam et al., "Development of a DNA-liposome complex for gene delivery applications," *C, Materials for Biological Applications*, vol. 75, pp. 191–197, 2017.

[44] L. T. Nguyen, K. Atobe, J. M. Barichello, T. Ishida, and H. Kiwada, "Complex formation with plasmid DNA increases the cytotoxicity of cationic liposomes," *Biological & Pharmaceutical Bulletin*, vol. 30, no. 4, pp. 751–757, 2007.